



## OPEN ACCESS

## EDITED BY

Zhi Li,  
Central South University, China

## REVIEWED BY

Huijun Wu,  
Guangzhou University, China  
Huaming Dai,  
Wuhan University of Technology, China  
Lunlun Gong,  
Hefei University of Technology, China

## \*CORRESPONDENCE

Weiwang Chen,  
✉ ww\_chen@cauc.edu.cn

## SPECIALTY SECTION

This article was submitted to Polymeric and Composite Materials, a section of the journal Frontiers in Materials

RECEIVED 07 November 2022

ACCEPTED 15 December 2022

PUBLISHED 18 January 2023

## CITATION

Jin Y, Tang Y, Cao W, Yan Y, Sun Y and Chen W (2023), Muscular kevlar aerogel tapes attractive to thermal insulation fabrics. *Front. Mater.* 9:1091830. doi: 10.3389/fmats.2022.1091830

## COPYRIGHT

© 2023 Jin, Tang, Cao, Yan, Sun and Chen. This is an open-access article distributed under the terms of the [Creative Commons Attribution License \(CC BY\)](https://creativecommons.org/licenses/by/4.0/). The use, distribution or reproduction in other forums is permitted, provided the original author(s) and the copyright owner(s) are credited and that the original publication in this journal is cited, in accordance with accepted academic practice. No use, distribution or reproduction is permitted which does not comply with these terms.

# Muscular kevlar aerogel tapes attractive to thermal insulation fabrics

YueYang Jin<sup>1</sup>, YaTing Tang<sup>1,2</sup>, WenHao Cao<sup>1</sup>, YangYang Yan<sup>1</sup>, Yueyan Sun<sup>1,2</sup> and Weiwang Chen<sup>2\*</sup>

<sup>1</sup>School of Safety Science and Engineering, Civil Aviation University of China, Tianjin, China, <sup>2</sup>Key Laboratory of Civil Aviation Thermal Hazards Prevention and Emergency Response, Civil Aviation University of China, Tianjin, China

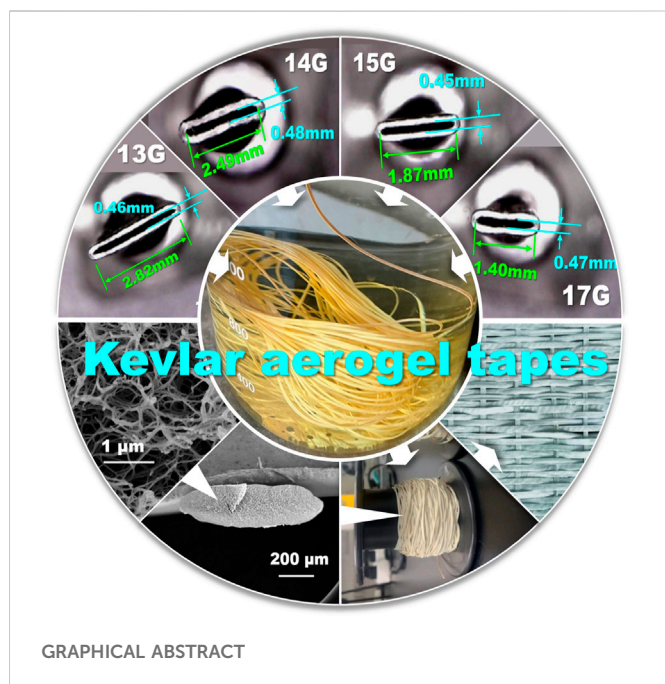
Kevlar aerogel is a kind of easy-casting nano-porous material with the characteristics of low density, high porosity, low thermal conductivity, high specific surface area, etc. It can serve as functional fibers and has a bright future in the field of thermal insulation after being processed into fabrics. To improve the tensile power of aerogel fibers to bear more loads while maintaining their flexibility for further braiding, a series of Kevlar aerogel tapes were fabricated in this study by using flattened needles. It is observed that the resultant aerogel tapes show a spindle-like cross section, and have greatly improved load-bearing capability with muscular tensile strength up to 2.07 MPa. The use of a larger needle is conducive to preparing aerogel tapes that are more attractive in load-bearing, and increasing Kevlar concentration tends to result in more muscular tapes with improved breaking stress but reduced elasticity. Besides, these tapes also inherit the excellent thermal stability and char-forming ability of Kevlar, starting to decompose at around 500°C and producing carbon residue more than 40% of their initial weight at 700°C. In addition, these Kevlar aerogel tapes also perform well in terms of thermal insulation. When exposed to a hot plate of 300°C, the fabric braided from these aerogel tapes show a considerable temperature drop per unit thickness as high as 120°C mm<sup>-1</sup>. It can be envisaged that the developed aerogel tapes with muscular tensile strength and their fabric products will be promising for high-temperature thermal insulation applications, such as being used as the insulation layer for thermal protective clothing.

## KEYWORDS

kevlar aerogel tape, flattened needle, freeze drying, thermal insulation, load-bearing capability

## 1 Introduction

Aerogel is a general term for nano-porous solid materials composed of colloidal particles or skeletons, which have ultralow density, impressive specific surface area and high porosity (Gurav et al., 2010; Lee and Park, 2020; Idumah et al., 2021). They are attractive as separation membranes, thermal insulators, high-efficient catalyst carriers, biosensors, etc., (Moreno-Castilla and Maldonado-Hódar, 2005; Cuce et al., 2014; Stergar and Maver, 2016; Jiang et al., 2022). Up to now, there are diverse kinds of aerogels available, generally classified into organic aerogels, inorganic aerogels, carbon aerogels and the composite ones (Guo et al., 2018; Alwin and Sahaya Shajan, 2020). Some of the aerogels can be processed into particles, thin films or flexible fibers, allowing them promising in thermal protective fabrics or even garments (Chang et al., 2014; Bhuiyan et al., 2020; Mekonnen et al., 2021; Tafreshi et al., 2022). Among them, the fabrics from organic polymer aerogel fibers are more appealing as they usually



perform better in terms of breathability, comfortable wearing and durability (Li et al., 2021; Liu et al., 2021).

Poly-*p*-phenylene terephthamide (PPTA, well known as Kevlar), a star polymer with excellent heat resistance, robust mechanical strength, inherent flame retardancy, etc., is widely used as the base material for fire protective clothing, insulation paper, heat-resistant filters, and so on (Zhang et al., 2018). It can be easily fabricated into aerogel fibers that can then be braided into fabrics (Li et al., 2019; Liu et al., 2019; An et al., 2021; Bao et al., 2021; Li et al., 2022a; Zuo et al., 2022). For example, Suzuki et al. (2019) prepared neat Kevlar aerogel fibers by sol-gel method followed by supercritical CO<sub>2</sub> drying, which presented outstanding flexibility and thermal insulation performance, implying that converting Kevlar into aerogel fibers is a benefit conduct (Suzuki et al., 2019). Li et al. (2022a) and Zuo et al. (2022) fabricated a series of flexible Kevlar aerogel fibers by a convenient wet-spinning technique and braided them into fabrics (Li et al., 2022a; Zuo et al., 2022). These aerogel fibers not only inherited most of the excellent properties of Kevlar, but also combined the advantages of aerogel, appealing for diverse applications. Liu et al. (2019) also utilized the same strategy to prepare Kevlar aerogel fibers and obtained similar fabrics that can be used in extreme environments (Liu et al., 2019). However, most of these aerogel fibers are ultrafine with diameters about 200–600 μm (Bao et al., 2021), expressed as quite small cross-sectional areas. This means that such aerogel fibers, despite their considerable tensile strength, cannot withstand relatively heavy loads. The ultrafine size of these Kevlar aerogel fibers together with their nano-porous structure gives them delicate mechanical properties that need to be further enhanced. It was reported that the mechanical enhancement of Kevlar aerogel fibers could be achieved by adding functional additives such as MXene (Lu et al., 2021; Zuo et al., 2022), carbon nanotubes (CNT) (Huang et al., 2022), etc., as well as introducing an extra sheath for support (Sun et al., 2021; Huang et al., 2022). But things are not always perfect, the strategies for enhancing mechanical properties of Kevlar aerogel fibers often come at the expense of deteriorating some other properties of the aerogel

fibers. For instance, the addition of MXene upgraded the thermal conductivity of Kevlar aerogels to about 86 mW·m<sup>-1</sup>·K<sup>-1</sup> (Zuo et al., 2022), which is much higher than the neat ones (~35 mW·m<sup>-1</sup>·K<sup>-1</sup>) (Liu et al., 2019; Li et al., 2022a), weakened performance in thermal insulation in other words. Given these, enlarging the cross section of the aerogel fibers may be another effective and easily accessible strategy to obtain muscular aerogel fibers with enhanced mechanical properties.

In this study, inspired by the rattan mat, we focus on fabricating muscular Kevlar aerogel tapes with a flat structure. This is to obtain a larger cross section than traditional aerogel fibers to bear more loads, meanwhile, to maintain their flexibility in the direction of thickness for further braiding. To achieve this, several flattened needles of different sizes were used, resulting in a series of Kevlar aerogel tapes. The structure, tensile properties and thermal behavior of the resultant aerogel tapes were characterized. The results reveal that all of the aerogel tapes have a spindle-like cross section, in accordance with what we pursued. The enlarged cross section attributes these aerogel tapes better load-bearing capability. Besides, these aerogel tapes also perform well in thermal insulation, better than the previously fabricated aerogel fibers. These advantages, combined with the inherent flame retardancy and appealing thermal stability of Kevlar, make the aerogel tapes attractive to thermal insulation fabrics.

## 2 Experimental details

### 2.1 Materials

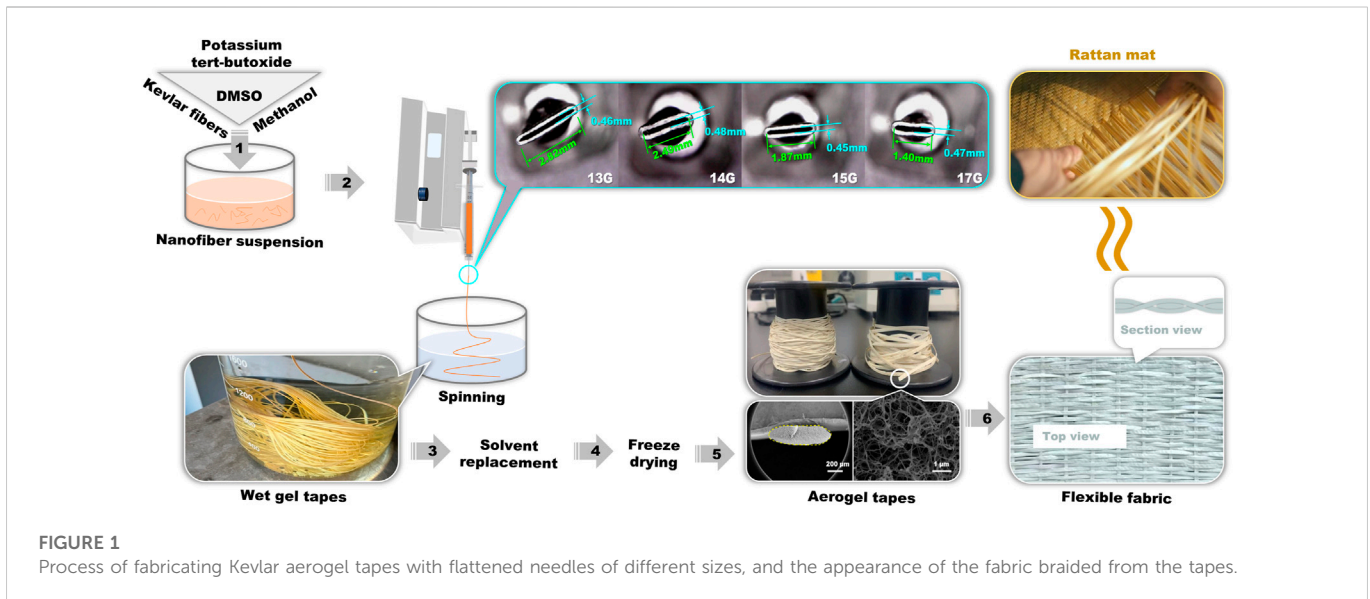
Commercial Kevlar fibers were supplied by Yantai Tayho Advanced Materials Co., Ltd. Dimethyl sulfoxide (DMSO), potassium tert-butoxide, methanol, and tert-butanol were purchased from Shanghai Aladdin Biochemical Technology Co. Ltd. The chemicals were used as received without further purification.

### 2.2 Preparation of spinning suspensions

Different suspensions for spinning with varying Kevlar concentrations of 4 wt.%, 6 wt.%, 8 wt.%, and 10 wt.% were prepared by dissolving a certain amount of commercial Kevlar fibers in DMSO with the help of potassium tert-butoxide and methanol, according to previous reports (Yang et al., 2011; Liu et al., 2019). The content of methanol in each suspension was set as 10 wt.%. To accelerate the dissolution of Kevlar fibers, continuous oven heating together with intermittent stirring was adopted.

### 2.3 Fabrication of aerogel tapes

The schematic diagram for fabricating Kevlar aerogel tapes is shown in Figure 1. To obtain Kevlar aerogel tapes of different sizes, four flattened needles born from 13 G, 14 G, 15 G and 17 G were used. The G here is short for gauge, reflecting the outside diameter of the needle. The larger the G value, the thinner the needle. After flattened, the outlets of these needles are approximately rectangular in shape. Their sizes are given in Figure 1; Supplementary Table S1 in the Supplementary Materials. As shown, the short sides of these needles are almost the same, about 0.45 mm, while the long sides are different



from each other, varying from 1.40 mm to 2.82 mm. In the process of spinning, the nanofiber suspensions of different Kevlar concentrations were extruded from a syringe reservoir into a coagulation water bath through one of the flattened needles given above. The feeding rate of the nanofiber suspension was set to be about proportional to the outlet area of the needle used, to ensure a relatively constant length of tape production. The suspension extruded was solidified gradually in the bath to form continuous flat wet gels. The wet gels were collected and were then extracted several times with 25 vol.% tert-butanol solutions to complete the solvent replacement. After that, the wet gels were refrigerated at  $-80^{\circ}\text{C}$  for about 24 h, and were then freeze-dried for 2 days to form aerogel tapes. For the convenience of discussion, the Kevlar aerogel tapes fabricated are marked as KAT-x-y, where x is the Kevlar concentration of the suspension used, and y is the needle used for wet-spinning.

## 2.4 Characterization

The cross-sectional appearance and microstructure of the resultant aerogel tapes were observed by using a ZEISS Sigma 500 field emission scanning electron microscopy (FE-SEM) under an accelerating voltage of 5 kV. Prior to the SEM observations, the samples were sputter-coated with gold to render them better electrical conductivity. The specific surface areas and pore size details of some aerogel tapes were obtained based on the Brunauer–Emmett–Teller (BET) theory of  $\text{N}_2$  adsorption method using a Mac ASAP 2460 multi-station analyzer as well as the Mercury intrusion porosimetry (MIP) using an AutoPore IV 9500 porosimeter. Their tensile properties were tested by an electronic universal testing machine of WDW-1M, with a gauge length of 100 mm and a loading rate of  $2\text{ mm}\cdot\text{min}^{-1}$ . Thermogravimetry (TG) analyses were conducted on a Mettler TGA/DSC3+ with a heating rate of  $10^{\circ}\text{C}\cdot\text{min}^{-1}$  from room temperature to  $700^{\circ}\text{C}$  in  $\text{N}_2$  atmosphere. In addition, these aerogel tapes were also braided into flexible fabrics, to further evaluate their performance in thermal insulation by placing them on a hot plate. The hot plate was heated from room temperature to a preset temperature of  $50^{\circ}\text{C}$ ,  $100^{\circ}\text{C}$ ,  $200^{\circ}\text{C}$ , or  $300^{\circ}\text{C}$ , to simulate high-temperature use scenarios.

The temperature differences between the outer surface of the fabric and the hot plate were recorded.

## 3 Results and discussion

### 3.1 Tap structure and morphology

At the very beginning, the size and cross-sectional appearance of the obtained aerogel tapes were characterized by SEM. The results are shown in Figure 2; Figure 3. It can be observed that the cross section of the aerogel tapes shows a spindle-like structure. The formation of the spindle-like section is mainly due to the difference in extrusion resistance, which is larger at both ends of the flattened needle. In other words, the spinning suspension at the ends suffers additional resistance from the short side of the needle to extrude. Therefore, it makes the extrusion of the spinning suspension more difficult at the ends than at the center of the needle, resulting in thinner tape thickness at the ends. These aerogel tapes with spindle-like sections are helpful for braiding compact fabrics with fewer and narrower air gaps between the tapes, making them more attractive for heat radiation shielding in thermal insulation applications.

The thickness and width of the resultant aerogel tapes are plotted in Figure 2. Each average tape width and tape thickness was calculated based on microscopic observations of at least ten samples. For the aerogel tapes fabricated with different needles but from the same spinning suspension of 4 wt.%, their thickness remains almost constant at about  $0.21\text{--}0.23\text{ mm}$ . This is because the needles used for fabrication have almost the same thickness. The width of these aerogel tapes, however, shows an increasing tendency from  $0.93 \pm 0.13\text{ mm}$  to  $1.40 \pm 0.13\text{ mm}$  as the needle used enlarges from 17 G to 13 G. For the aerogel tapes obtained with the same needle but from varying spinning suspensions of different Kevlar concentrations, their width is nearly the same while their thickness increases gradually with the increase of Kevlar concentration. The increase in thickness can be explained by the Barus effect (Goto et al., 1986; Liang, 2008). That is, polymer solutions tend to swell as they are extruded from a die, and

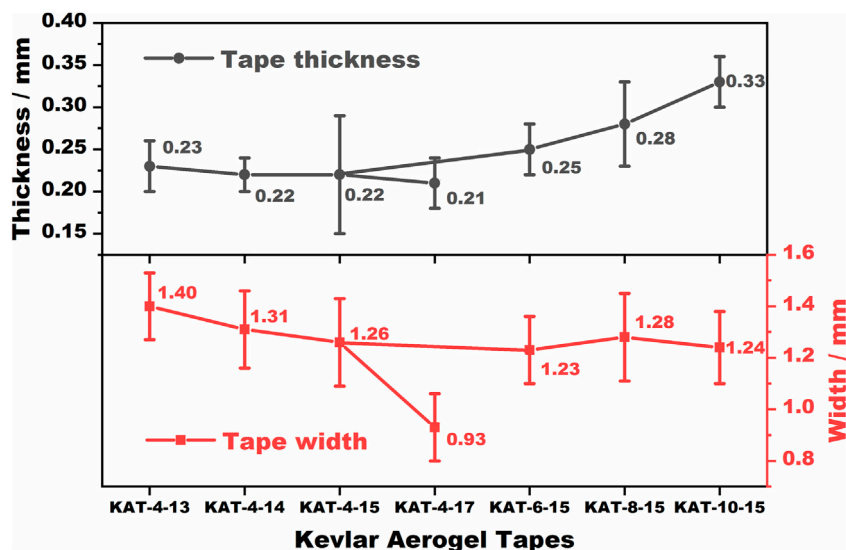


FIGURE 2 The thickness and width of the resultant aerogel tapes.

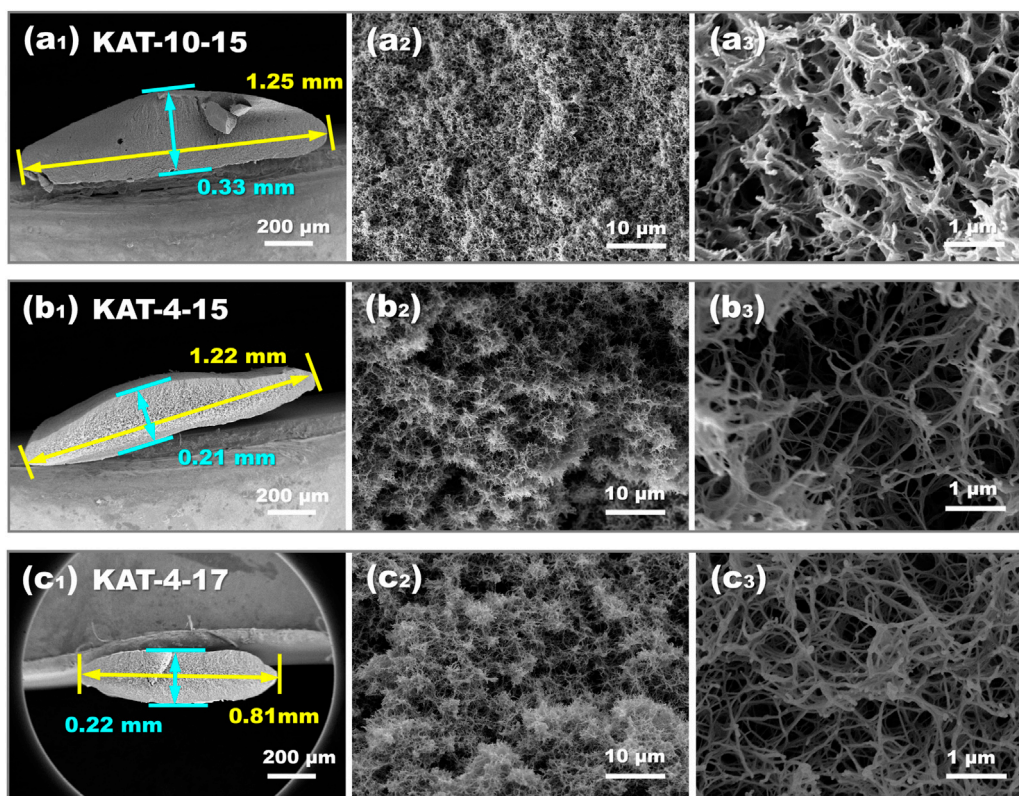


FIGURE 3 The size and microstructure of several representative Kevlar aerogel tapes observed by SEM: (A) KAT-10-15, (B) KAT-4-15, and (C) KAT-4-17.

tend to swell more when a more viscous solution with a higher polymer concentration is used. It is thus reasonable to obtain thicker aerogel tapes from a higher Kevlar concentration.

From the above analyses, it can be given that the size of the aerogel tapes is mainly determined by the needle used. This also means that a wide variety of Kevlar aerogel tapes can be fabricated by customizing

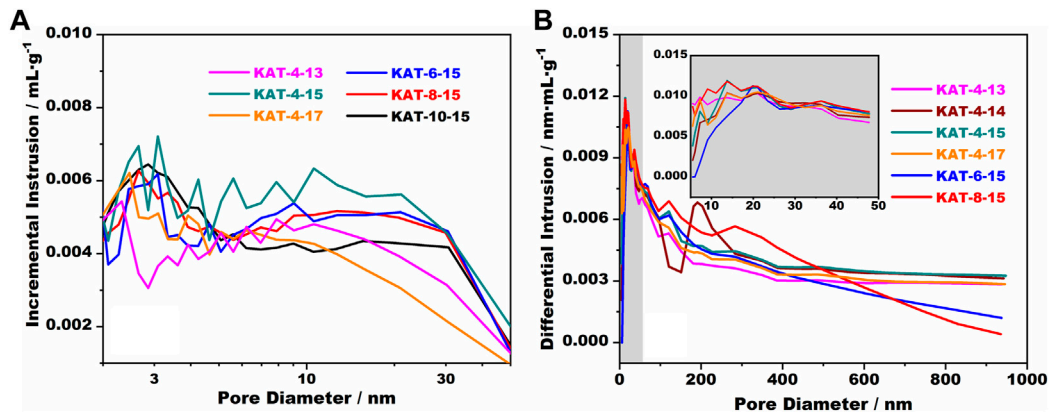


FIGURE 4 Pore size details of the resultant aerogel tapes given by the methods of (A)  $N_2$  adsorption and (B) MIP.

spinning needles of desired shape and size. Even so, the cross-sectional deformation and the severe shrinkage of the aerogel tapes cannot be ignored. As shown in Figure 2; Supplementary Table S1 in the Supplementary Materials, the width and thickness of the obtained tapes are apparently much smaller than the size of the needle used, with some even half the size. The shrinkage they suffered in the process of entire fabrication, especially during freeze drying should be responsible.

The SEM images in Figure 3 show that the aerogel tapes are all porous in structure, which contributes to their ultralow density ( $0.05\text{--}0.29\text{ g}\cdot\text{cm}^{-3}$ ), high specific surface areas ( $117.15\text{--}157.95\text{ m}^2\cdot\text{g}^{-1}$  by MIP), and high porosity ( $81.4\%\text{--}94.8\%$  by MIP). In contrast, the surface of the tapes prepared is relatively smooth and compact. For more details, please refer to Supplementary Table S1; Supplementary Figure S1 in the Supplementary Materials. Among these aerogel tapes, KAT-10-15 in Figure 3A fabricated from the highest Kevlar concentration of 10 wt.% shows a relatively denser nanofibrous structure with the highest density of  $0.29\text{ g}\cdot\text{cm}^{-3}$ , but has severe fiber conglutination issue. This could probably be a good thing as fiber conglutination is beneficial for mechanical improvement, somewhat similar to that of muscular polyimide aerogels dried by supercritical ethanol (Chen et al., 2022). The BET specific surface area of KAT-10-15 was measured to be  $135.5\text{ m}^2\cdot\text{g}^{-1}$ . Its pore size details, together with those of some other aerogel tapes, are plotted in Figure 4. The results indicate that, in addition to the macropores with diameters of hundreds of nanometers observed by SEM, there are also a large number of mesopores in KAT-10-15, as well as in the other aerogel tapes. In other words, the porous structure of Kevlar aerogel tapes is multi-layered, assembled by numerous pores ranging from several to hundreds of nanometers. This is appealing to thermal insulation, as these small pores especially the nano-sized ones can provide the tapes with negligible gaseous convection and reduced conduction by greatly restricting the motion of gas molecules. For KAT-4-15 fabricated from a lower Kevlar concentration of 4 wt.%, it is more loosely assembled than KAT-10-15. It is observed that the nanofibers in KAT-4-15 are jointed together, but separate from each other with almost no fiber conglutination. The difference in microstructure will inevitably bring these aerogel tapes observable differences in mechanical strength and some other properties.

By further comparing KAT-4-15 with the KAT-4-17 shown in Figure 3C, the tape extruded from a needle of smaller width also shows a relatively denser nanofiber structure. But the microstructure of KAT-4-17 is not very different from that of KAT-4-15, i.e., the effect of needle size on the tape's microstructure is limited. It therefore is possible to design and cast size-adjustable Kevlar aerogel tapes by using spinning needles of different sizes, while to regulate the tape's microstructure by using spinning suspensions of different Kevlar concentrations.

### 3.2 Tensile properties

As mentioned above, this study focuses on enhancing the tensile strength of aerogel fibers by fabricating them into aerogel tapes. This is achieved by enlarging the cross-sectional area to offer them muscular ability in load-bearing, so as to facilitate their processing and use. The tensile properties of the as-fabricated aerogel tapes were investigated, with the results shown in Figure 5. The abscissa, i.e., strain, represents the axial deformation degree of the tape, expressed as elongation in this study. It can be seen from Figure 5A1 that the maximum force that the tape can bear increases gradually from 0.45 N to 0.89 N with the increase of tape width. This indicates that the tensile power of the aerogel tapes was largely improved by increasing the area to bear the load, which is consistent with our original intention. For their stress-strain curves in Figure 5A2, however, there appears a tendency for the stress at break to decrease first and then increase as the tape width decreases gradually. Nevertheless, these curves show almost the same slope. Their difference in breaking stress is mainly because they break at different elongations. If we assume the elongation to be the same, the breaking stress of these aerogel tapes from the same spinning suspension but with different needles should be close to each other. This points the direction for our future work, to further optimize the stability of aerogel tapes in mechanical performance. The tensile strength of these aerogel tapes in the present study is still comparable to or higher than that of the Kevlar aerogel fibers reported previously. For example, the aerogel tape of KAT-4-15 shows breaking stress of 1.05 MPa, which is higher than the 0.55–0.86 MPa of the corresponding aerogel fibers prepared by using an un-flattened spinning needle (Sun et al., 2021), and is

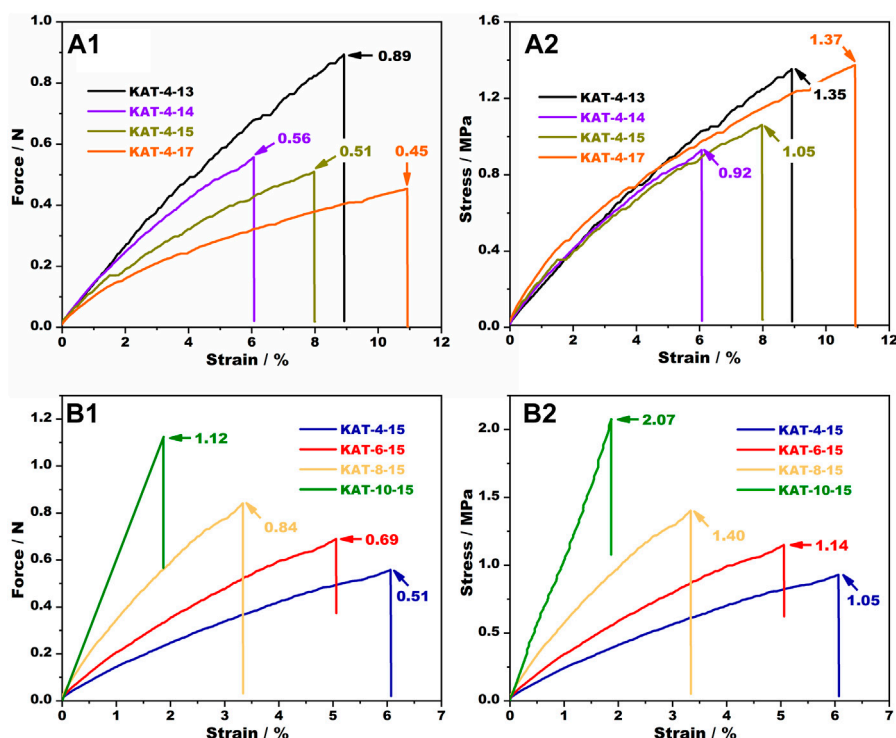


FIGURE 5

The force-strain and stress-strain curves of the resultant aerogel tapes fabricated with (A) different needles and (B) from different spinning suspensions with varying Kevlar concentrations.

comparable to those reported by Li et al. (2019), Liu et al. (2019) If the elongation of the current aerogel tapes can be as long as that of the previously reported Kevlar aerogel fibers, the tape's breaking stress will be much higher. Unfortunately, this is not the case. Even so, the enlarged cross section allows these aerogel tapes to bear more load, as a larger cross-sectional area means the tape has more units, i.e., Kevlar nanofibers, for load-bearing. For practical applications, the prepared aerogel tapes with better bearing capacity can withstand relatively high shock and are not easily to be broken. As to the shape changes of the aerogel tape after tensile test, it was observed that the cross section of the tape was distorted and no longer regular as before (see Supplementary Figure S2 in the Supplementary Materials). The tape after tensile test was reduced in width and thickness, which was caused by stretching.

When it comes to the aerogel tapes obtained with the same needle but from different spinning suspensions, the force they can bear at break shows a gradual increase from 0.51 N to 1.12 N as Kevlar concentration increases from 4 wt.% to 10 wt.%, as shown in Figure 5B1. This is quite easy to understand because a higher Kevlar concentration means there will be more nanofibers per unit area of the tape to against external tensile force, expressed as greater force at break. Besides, the severe conglutination among nanofibers at high Kevlar concentrations may also be beneficial to enhance the load-bearing capacity of the aerogel tapes. If we further convert these force-strain curves into the classical stress-strain ones with stress as the ordinate, the trend for stress is the same as that for force. That is, the breaking stress of these aerogel tapes increases gradually as Kevlar concentration increases. The results show that the breaking stress of KAT-10-15 is as high as 2.07 MPa, almost twice that of KAT-4-15.

But the elongation of KAT-10-15 at break is shortened, indicative of a significant degradation in elasticity. It can be given that the higher the concentration of Kevlar, the more muscular but more rigid the aerogel tapes will be.

From the above discussion, there are reasons to believe that using spinning needle of a larger size is conducive to preparing aerogel tapes that perform better in load-bearing, and increasing Kevlar concentration will result in more muscular tapes with improved breaking stress but reduced elasticity. Aerogel tapes with different tensile properties thereby can be customized by adjusting the needle size and Kevlar concentration. To obtain Kevlar aerogel tapes with muscular tensile strength without considering their elasticity, a relatively larger needle together with a higher polymer concentration is preferred for spinning.

### 3.3 Thermal behavior

To investigate the thermal decomposition performance of the aerogel tapes, TG analysis was conducted. The results are shown in Figure 6. It can be seen from the figure that the aerogel tapes from different Kevlar concentrations show almost the same behavior in thermal decomposition. One of the main differences among them lies in the amount of volatiles they contain, including the moisture absorbed as well as the solvents remained, which are removed before 130°C. Thereafter, these aerogel tapes almost do not continue to decompose until the temperature reaches about 500°C, indicative of outstanding performance in thermal stability. As can be seen from the enlarged TG curves in Figure 6, the temperatures at

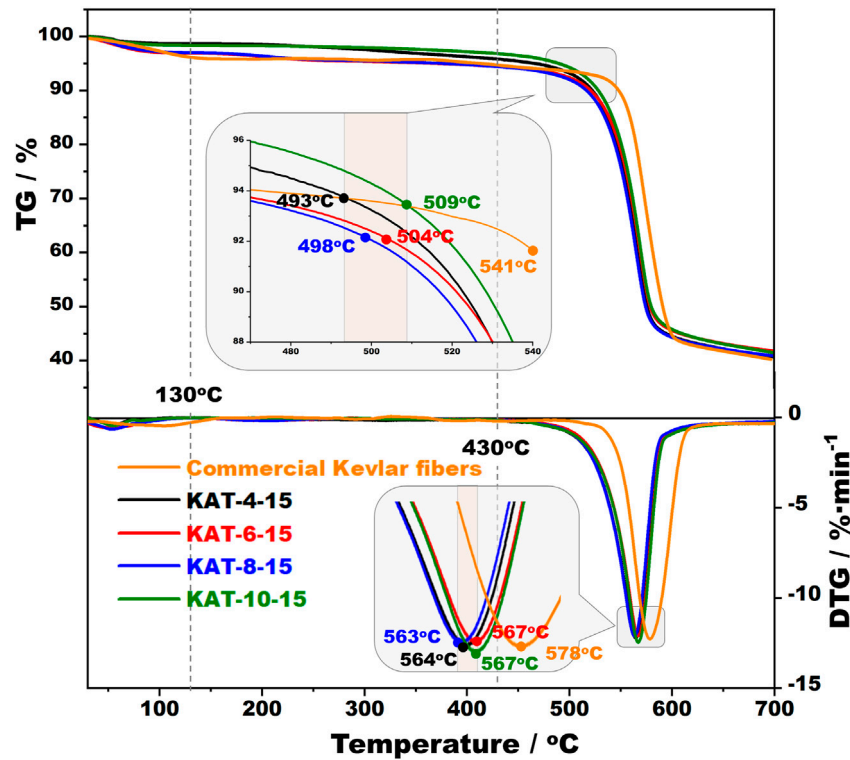


**FIGURE 6**  
TG and DTG curves of commercial Kevlar fibers and the aerogel tapes fabricated from different Kevlar concentrations.

which these tapes suffer a 5% mass loss of their solid contents vary from 493°C to 509°C, only about 30°C lower than that of commercial Kevlar fibers. The corresponding derivative thermogravimetry (DTG) curves of these four aerogel tapes also show maximum weight loss rates at about 565°C, slightly lower than that of commercial Kevlar fibers as well. All of these confirm that the excellent thermal stability of Kevlar is well retained after being processed into aerogel tapes.

More than that, the carbon residue of the aerogel tapes remained at 700°C are beyond 40% of their initial weight. This is also crucial for high-temperature thermal insulation applications, as the pyrolytic carbon residue usually deserves a porous structure (Choma et al., 2016), which can further endow the polymer with better flame retardancy and can better shield the objects protected to reduce heat injury. The outstanding performance of Kevlar aerogel tapes in char-forming and thermal stability contribute to their great potential for high-temperature applications.

The thermal insulation performance of the resultant aerogel tapes was then evaluated preliminarily by braiding them into fabrics, followed by placing the fabric on a hot plate of different temperatures. The hot plate was set to 50°C, 100°C, 200°C and 300°C in sequence. The front view of the fabric can be seen in Figure 1. Compared with our previous fabrics braided from consanguineous aerogel fibers (Sun et al., 2021), the current fabric from Kevlar aerogel tapes looks more like a rattan mat, and seems to be more tightly braided with fewer and narrower air gaps formed between adjacent tapes. This brings such fabrics better shielding against thermal radiation, and thereby may endow their better performance in thermal insulation.

Figure 7 plots the outer surface temperatures of the fabrics braided from KAT-4-15 and KAT-4-13 over time at different exposure temperatures. It is apparent that the outer surface temperatures of these two aerogel fabrics are both lower than that of the hot plate. When the hot plate was set to 300°C, for example, the temperature difference between the fabric and the hot plate could be up to 70°C, resulting in a considerable temperature drop per unit thickness of about 120°C mm<sup>-1</sup>. The temperature drop is much higher than that of some previously reported Kevlar aerogel fibers including our coaxial ones (Sun et al., 2021; Li et al., 2022a; Li et al., 2022b). This indicates that the current aerogel tapes indeed performed better in thermal insulation than the aerogel fibers that were mechanically enhanced by introducing a Nomex shell. The thermal conductivity of a similar but much wider KAT-4-year aerogel tape is tested to be only 37 mW·m<sup>-1</sup>·K<sup>-1</sup> by using a Hot Disk TPS2500 apparatus, while those for KAT-6-year and KAT-8-year are 40.8 mW·m<sup>-1</sup>·K<sup>-1</sup> and 45.3 mW·m<sup>-1</sup>·K<sup>-1</sup>, respectively. Besides, the outer surface temperature of the fabric braided from KAT-4-15 was also observed to be lower than that of the other fabric braided from KAT-4-13 throughout the entire heating and cooling process. Their difference in tape size and thereby fabric thickness should be responsible. The SEM images in Figure 3 show that the aerogel tapes have a spindle-like cross section, whose ends tend to be sharper as the needle size enlarges. The sharper the ends of the tape's cross section, the thinner the fabric tends to be. Not only that, increasing the number of aerogel tapes per unit length means more bends to form a fabric, which is also conducive to increasing the thickness of the fabric. The aerogel tapes of KAT-4-15 thereby tend to be braided into a relatively thicker fabric, whose thickness is measured to be about 0.58 mm,

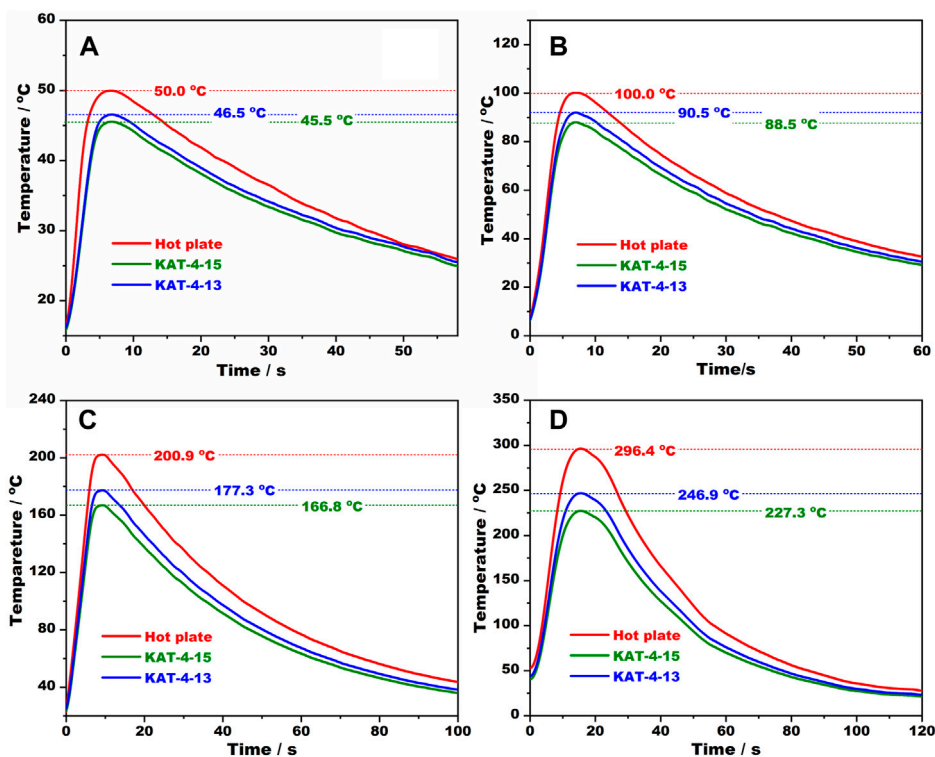


FIGURE 7

The variations of the outer surface temperature of the aerogel fabrics, placed on a hot plate of different temperatures: (A) 50°C, (B) 100°C, (C) 200°C and (D) 300°C.

indeed slightly thicker than the other fabric from KAT-4-13. It therefore makes sense that the fabric braided from KAT-4-15 performs better in thermal insulation.

## 4 Conclusion

In this study, a series of Kevlar aerogel tapes were fabricated using flattened needles of different sizes based on the coupled strategy of wet-spinning and freeze drying. The structure, tensile properties and thermal behavior of the obtained aerogel tapes were characterized. It is observed that the aerogel tapes have a nano-porous structure assembled by numerous nanofibers, and show a spindle-like cross section with a thick center and narrow ends. Thanks to the enlarged cross section by using flattened needles and the bushier branches gained from denser spinning suspensions to bear more load, these aerogel tapes show greatly improved load-bearing capability with muscular tensile strength. Besides, the excellent thermal stability and char-forming performance of Kevlar are also well preserved after being processed into aerogel tapes. The onset temperatures of these tapes to decompose are still around 500°C, with carbon residue more than 40% of their initial weight produced at 700°C. In addition, these Kevlar aerogel tapes also perform well in thermal insulation. The thermal insulation performance of the fabric depends on its thickness to a large extent and is closely related to the size of the needle used. The outer surface temperature of the fabric braided from KAT-4-15 can be 70°C lower than that of the hot plate, resulting in a considerable temperature drop per unit thickness of about 120°C mm<sup>-1</sup> when exposed to 300°C. Given these, the developed aerogel tapes with muscular tensile

strength, inherent flame retardancy and appealing thermal stability may have great appeal in flexible and survivable fabrics for thermal insulation at high temperatures.

## Data availability statement

The original contributions presented in the study are included in the article/Supplementary Material, further inquiries can be directed to the corresponding author.

## Author contributions

All the authors contributed to the design of this study and the writing of this manuscript. YJ, WC, and YY performed the experiments and worked in the data curation. YS, and YT performed the statistical analysis and the data visualization. WC reviewed and edited, and all the author agreed to the final version of the manuscript.

## Funding

This work was supported by National Natural Science Foundation of China (51904312), Applied Foundational Research Funds of Tianjin Province (21JCQNJC00740), Fundamental Research Funds for the Central Universities (3122022100), Scientific Research Foundation of Civil Aviation University of China (2020KYQD115), and National

Undergraduate Training Program for Innovation and Entrepreneurship (202110059026).

## Acknowledgments

The authors are deeply grateful to these supports.

## Conflict of interest

The authors declare that the research was conducted in the absence of any commercial or financial relationships that could be construed as a potential conflict of interest.

## References

- Alwin, S., and Sahaya Shajan, X. (2020). Aerogels: Promising nanostructured materials for energy conversion and storage applications. *Mater. Renew. Sustain. Energy* 9, 7. doi:10.1007/s40243-020-00168-4
- An, L., Liang, B., Guo, Z., Wang, J., Li, C., Huang, Y., et al. (2021). Wearable Aramid-ceramic aerogel composite for harsh environment. *Adv. Eng. Mater.* 23, 2001169. doi:10.1002/adem.202001169
- Bao, Y., Lyu, J., Liu, Z., Ding, Y., and Zhang, X. (2021). Bending stiffness-directed fabricating of Kevlar aerogel-confined organic phase-change fibers. *ACS Nano* 15, 15180–15190. doi:10.1021/acsnano.1c05693
- Bhuiyan, M. A. R., Wang, L., Shaid, A., Jahan, I., and Shanks, R. A. (2020). Silica aerogel-integrated nonwoven protective fabrics for chemical and thermal protection and thermophysiological wear comfort. *J. Mater. Sci.* 55, 2405–2418. doi:10.1007/s10853-019-04203-2
- Chang, K., Wang, Y., Peng, K., Tsai, H., Chen, J., Huang, C., et al. (2014). Preparation of silica aerogel/polyurethane composites for the application of thermal insulation. *J. Polym. Res.* 21, 338. doi:10.1007/s10965-013-0338-7
- Chen, W., Liu, S., Sun, Y., Zhou, X., and Zhou, F. (2022). Melamine-crosslinked polyimide aerogels from supercritical ethanol drying with improved in-use shape stability against shrinking. *Macromol. Mater. Eng.* 307, 2100645. doi:10.1002/mame.202100645
- Choma, J., Osuchowski, L., Marszewski, M., Dziura, A., and Joniec, M. (2016). Developing microporosity in Kevlar<sup>®</sup>-derived carbon fibers by CO<sub>2</sub> activation for CO<sub>2</sub> adsorption. *J. CO<sub>2</sub> Util.* 16, 17–22. doi:10.1016/j.jcou.2016.05.004
- Cuce, E., Cuce, P. M., Wood, C. J., and Riffat, S. B. (2014). Toward aerogel based thermal superinsulation in buildings: A comprehensive review. *Renew. Sustain. Energy Rev.* 34, 273–299. doi:10.1016/j.rser.2014.03.017
- Goto, S., Nagazono, H., and Kato, H. (1986). The flow behavior of fiber suspensions in Newtonian fluids and polymer solutions. *Rheol. Acta* 25, 119–129. doi:10.1007/BF01332131
- Guo, F., Jiang, Y., Xu, Z., Xiao, Y., Fang, B., Liu, Y., et al. (2018). Highly stretchable carbon aerogels. *Nat. Commun.* 9, 881. doi:10.1038/s41467-018-03268-y
- Gurav, J. L., Jung, I. K., Park, H. H., Kang, E. S., and Nadargi, D. Y. (2010). Silica aerogel: Synthesis and applications. *J. Nanomater.* 2010, 1–11. doi:10.1155/2010/409310
- Huang, J., Li, J., Xu, X., Hua, L., and Lu, Z. (2022). *In situ* loading of polypyrrole onto Aramid nanofiber and carbon nanotube aerogel fibers as physiology and motion sensors. *ACS Nano* 16, 8161–8171. doi:10.1021/acsnano.2c01540
- Idumah, C. I., Ezika, A. C., and Okpechi, V. U. (2021). Emerging trends in polymer aerogel nanoarchitectures, surfaces, interfaces and applications. *Surfaces Interfaces* 25, 101258. doi:10.1016/j.surfin.2021.101258
- Jiang, Y., Zhang, Y., Gao, C., An, Q., Xiao, Z., and Zhai, S. (2022). Superhydrophobic aerogel membrane with integrated functions of biopolymers for efficient oil/water separation. *Sep. Purif. Technol.* 282, 120138. doi:10.1016/j.seppur.2021.120138
- Lee, J., and Park, S. (2020). Recent advances in preparations and applications of carbon aerogels: A review. *Carbon* 163, 1–18. doi:10.1016/j.carbon.2020.02.073
- Li, J., Wang, J., Wang, W., and Zhang, X. (2019). Symbiotic aerogel fibers made via *in situ* gelation of Aramid nanofibers with polyamidoxime for uranium extraction. *Molecules* 24, 1821. doi:10.3390/molecules24091821
- Li, M., Chen, X., Li, X., Dong, J., Teng, C., Zhao, X., et al. (2022). Ultralight aerogel textiles based on aramid nanofibers composites with excellent thermal insulation and electromagnetic shielding properties. *Compos. Commun.* 35, 101346. doi:10.1016/j.coco.2022.101346
- Li, M., Chen, X., Li, X., Dong, J., Zhao, X., and Zhang, Q. (2022). Controllable strong and ultralight Aramid nanofiber-based aerogel fibers for thermal insulation applications. *Adv. Fiber Mater.* 4, 1267–1277. doi:10.1007/s42765-022-00175-2
- Li, X., Dong, G., Liu, Z., and Zhang, X. (2021). Polyimide aerogel fibers with superior flame resistance, strength, hydrophobicity, and flexibility made via a universal sol-gel confined transition strategy. *ACS Nano* 15, 4759–4768. doi:10.1021/acsnano.0c09391
- Liang, J. (2008). Effects of extrusion conditions on die-swell behavior of polypropylene/diatomite composite melts. *Polym. Test.* 27, 936–940. doi:10.1016/j.polymertesting.2008.08.001
- Liu, Y., Zhang, Y., Xiong, X., Ge, P., Wu, J., Sun, J., et al. (2021). Strategies for preparing continuous ultraflexible and ultrastrong poly(vinyl alcohol) aerogel fibers with excellent thermal insulation. *Macromol. Mater. Eng.* 306, 2100399. doi:10.1002/mame.202100399
- Liu, Z., Lyu, J., Fang, D., and Zhang, X. (2019). Nanofibrous Kevlar aerogel threads for thermal insulation in harsh environments. *ACS Nano* 13, 5703–5711. doi:10.1021/acsnano.9b01094
- Lu, Z., Jia, F., Zhuo, L., Ning, D., Gao, K., and Xie, F. (2021). Micro-porous MXene/Aramid nanofibers hybrid aerogel with reversible compression and efficient EMI shielding performance. *Compos. Part B Eng.* 217, 108853. doi:10.1016/j.compositesb.2021.108853
- Mekonnen, B. T., Ding, W., Liu, H., Guo, S., Pang, X., Ding, Z., et al. (2021). Preparation of aerogel and its application progress in coatings: A mini overview. *J. Leather Sci. Eng.* 3, 25. doi:10.1186/s42825-021-00067-y
- Moreno-Castilla, C., and Maldonado-Hódar, F. J. (2005). Carbon aerogels for catalysis applications: An overview. *Carbon* 43, 455–465. doi:10.1016/j.carbon.2004.10.022
- Stegar, J., and Maver, U. (2016). Review of aerogel-based materials in biomedical applications. *J. Sol-Gel Sci. Technol.* 77, 738–752. doi:10.1007/s10971-016-3968-5
- Sun, Y., Chen, W., and Zhou, X. (2021). Thermal insulation fibers with a Kevlar aerogel core and a porous Nomex shell. *RSC Adv.* 11, 34828–34835. doi:10.1039/D1RA06846F
- Suzuki, Y., Uchimura, A., Tabata, I., Uematsu, H., Hori, T., and Hirogaki, K. (2019). Preparation of *para*-Aramid aerogel fiber through physical gelation of Aramid dispersion liquid and supercritical drying. *AATCC J. Res.* 6, 28–32. doi:10.14504/ajr.6.S1.6
- Tafreshi, O. A., Mosanenzadeh, S. G., Karamikamkar, S., Saadatnia, Z., Park, C. B., and Naguib, H. E. (2022). A review on multifunctional aerogel fibers: Processing, fabrication, functionalization, and applications. *Mater. Today Chem.* 23, 100736. doi:10.1016/j.mtchem.2021.100736
- Yang, M., Cao, K., Sui, L., Qi, Y., Zhu, J., Waas, A., et al. (2011). Dispersions of aramid nanofibers: A new nanoscale building block. *ACS Nano* 5, 6945–6954. doi:10.1021/nn2014003
- Zhang, Z., Lee, N., Patel, K., Young, M., Zhang, J., Percec, S., et al. (2018). Poly(p-phenylene terephthalamide) fibers reinforced with ultrathin ceramic coatings. *Adv. Eng. Mater.* 20, 1800095. doi:10.1002/adem.201800095
- Zuo, X., Fan, T., Qu, L., Zhang, X., and Miao, J. (2022). Smart multi-responsive aramid aerogel fiber enabled self-powered fabrics. *Nano Energy* 101, 107559. doi:10.1016/j.nanoen.2022.107559

## Publisher's note

All claims expressed in this article are solely those of the authors and do not necessarily represent those of their affiliated organizations, or those of the publisher, the editors and the reviewers. Any product that may be evaluated in this article, or claim that may be made by its manufacturer, is not guaranteed or endorsed by the publisher.

## Supplementary material

The Supplementary Material for this article can be found online at: <https://www.frontiersin.org/articles/10.3389/fmats.2022.1091830/full#supplementary-material>